

A statistical study of Pc3-Pc5 magnetic pulsations observed by the AMPTE/Ion Release Module satellite

M. R. Lessard¹ and M. K. Hudson

Department of Physics and Astronomy, Dartmouth College, Hanover, New Hampshire

H. Lühr

GeoForschungsZentrum, Potsdam, Germany

Abstract. Magnetic field data from the Active Magnetospheric Particle Tracer Explorers/Ion Release Module satellite are used to complete a statistical study yielding occurrence rates of a number of different types of pulsations. Two hour panels of dynamic spectra and detrended line plots were inspected to determine occurrence rates over all local times from $L = 6$ to $L = 20$. Event types include fundamental field line resonances, harmonic resonances, storm time pulsations, and signatures of bursty bulk flows and fast flows. However, we also include observations of Pc3 compressional pulsations and note their association with harmonic events. Likewise, we include high-frequency events (40–70 mHz) and show a relation to storm time pulsations. On the basis of the occurrence distributions, we are able to make a number of conclusions. We determine that the excitation source of fundamental resonances is likely band limited from 3 to 10 mHz and that harmonic resonances are at least sometimes associated with compressional Pc3 pulsations. Storm time pulsations, compressional in nature, are sometimes associated with relatively high frequency transverse events and often occur in regions very close to the magnetopause. On the basis of other works that associate these pulsations with instabilities in the partial ring current, we suggest that particles that form the partial ring current may extend to the magnetopause during storms and substorms. Finally, we note that bursty bulk flows and fast flows in general have a magnetic signature that is predominantly compressional, and we discuss the relevance this may have regarding substorm dipolarization.

1. Introduction

A number of statistical studies of the magnetosphere using both ground-based and satellite data have been completed which have proven to be very useful in understanding generation mechanisms of various types of pulsations. In this work, we report results of a statistical survey of occurrence rates of signals with periods in the Pc3–Pc5 range (10–600 s) observed by the Active Magnetospheric Particle Tracer Explorers/Ion Release Module (AMPTE/IRM) satellite. We consider events of various types (and, presumably, different excitation mechanisms) and define these types on the basis of previous reports of observations and theory. While some

events such as fundamental and harmonic resonances appear to be very well understood, other activity such as that associated with bursty bulk flows has been studied much less. Not all of the events we include are necessarily coherent pulsations. For example, signals with compressional oscillations that may be associated bursty bulk flows do not appear to result from wave activity. These are included in this study because their occurrence distribution may be helpful in understanding their origins even if they are not wave related.

Statistical surveys have been completed using data sets from many different satellites with different orbits. A number of studies have investigated fundamental and harmonic field line resonances using geosynchronous data [Junginger et al., 1984; Kokubun, 1985; Kokubun et al., 1989; Takahashi and McPherron, 1984]. Anderson et al. [1990] used AMPTE/CCE data and Cao et al. [1994] used ISEE 1 data, both with elliptical orbits, to extend survey results to larger L shells near the equator. More recently, data from polar orbiting satellites have also been used for statistical analysis. Nosé et al. [1995]

¹Now at Institute for Space Research, Department of Physics and Astronomy, University of Calgary, Calgary, Alberta, Canada.

used magnetic field data from DE 1 and *Potemra and Blomberg* [1996] used magnetic and electric field data from Viking to investigate characteristics of resonances at high latitudes.

Other studies have focused on compressional oscillations. As with observations of resonances, earlier surveys used data from geosynchronous satellites [*Barfield and McPherron*, 1972; *Higuchi and Kokubun*, 1988; *Kokubun*, 1985; *Takahashi et al.*, 1985], while other studies (mostly later) used data from satellites with elliptical orbits [*Anderson et al.*, 1990; *Cao et al.*, 1994; *Hedgecock*, 1976; *Zhu and Kivelson*, 1991] and polar orbits [*Potemra and Blomberg*, 1996]. While the majority of these studies considered the relationship between magnetic storms and compressional pulsations, *Anderson et al.* [1990] took a more general approach by separating compressional signatures associated with storms from those with different origins. They were then able to show a peak in the occurrence rate distribution of non-storm-time compressional pulsations on the dayside. *Zhu and Kivelson* [1991] recorded mean wave amplitudes observed by ISEE 1 and 2 in the day-side magnetosphere, and they suggest that pulsations occurring on the dawn and dusk flanks are excited by internal plasma instabilities. The relationship of their study to others is difficult to reconcile, however, because the relationship between mean wave amplitudes and occurrence rates is not known.

Coherent pulsations constitute only one of several possible sources of signals in the Pc3-Pc5 frequency range. Other activity can also modulate the magnetic field at these frequencies, although their signals tend to be more broadband. Transient events can be observed in the day-side magnetosphere [*Sanmy et al.*, 1996] and in the night-side [*Takahashi et al.*, 1996]. Fluctuations associated with substorms such as neutral sheet oscillations [*Bauer et al.*, 1995], low-frequency oscillations at substorm breakup [*Holter et al.*, 1995], and signals associated with Pi2 onset [*Saka et al.*, 1996] are common. *Kokubun* [1983] showed that magnetic signatures of storm sudden commencements are detected at geosynchronous orbit over a broad range in local time, from 0300 to 2100. All of these incoherent types (and, undoubtedly, others not listed) contribute to the spectral signatures in the plots we considered. By defining a list of event types with clear signatures, we believe we have significantly reduced the amount of contamination from unwanted events in our study.

2. AMPTE/IRM Trajectory and Magnetic Field Experiment

The AMPTE/IRM satellite was launched on August 16, 1984, into an elliptical orbit with an apogee of approximately $18.8 R_E$ and a perigee of 557 km. The orbit, with a period of 44.3 hours, was inclined 28.6° from the geographic equator and precessed westward 23.0 hours in local time per year (0.95° per day). Mag-

netic field data were obtained using a three-axis fluxgate magnetometer mounted at the end of a 2 m carbon fiber boom [*Lühr et al.*, 1985], and sampled at 32 samples per second, although spin-averaged data (4.5 s period) were used for this study. The magnetometer was capable of operating in two ranges and was controlled automatically, but for the data we considered it was always operated in the higher-resolution mode of 0.12 nT.

Because the satellite's orbit was highly elliptical, its speed through regions in the $L = 6 - 9$ range was very fast, typically crossing $\Delta L = 1$ in 40 min or less and resulting in limited sampling of inner L shells. In addition, the relatively high inclination combined with the dipole tilt provided latitudinal coverage of approximately $\pm 40^\circ$. The combination of broad latitudinal coverage and high satellite speeds resulted in sampling intervals with inadequate latitudinal information for a statistical survey. For this reason, we consider occurrence rates in only two dimensions, L shell and magnetic local time.

This survey was completed with the goal of determining occurrence rates of pulsations in the regions from $L = 6$ to the magnetopause. Our results should overlap those of *Anderson et al.* [1990], although the coverage of inner L shells provided by AMPTE/CCE is significantly better. Our intention has been, in part, to extend their results to magnetospheric regions beyond AMPTE/CCE apogee, which occurred near $L = 9$. In order to exclude events in the magnetosheath, we use a conservative definition for detection of the magnetopause, similar to that used by *Zhu and Kivelson* [1991]. If the satellite is on the outbound leg of its orbit, we ignore data beyond the point where the plasma velocity exceeds 100 km/s the first time. If the satellite is inbound, we consider data only after the plasma velocity has dropped below 100 km/s for the last time.

Figure 1 shows observation times as a function of L shell and magnetic local time. Bins having a total of 2 hours or less are cross hatched, and occurrence rates in these bins are not calculated because of the poor statistics. The average position of the magnetopause [*Holzer and Slavin*, 1978] is plotted as a solid line, and regions beyond this line are typically cross hatched because of the above requirement that the satellite be within the magnetopause, resulting in little or no observation time for these bins. The clear increase in times for larger L shells results from the large apogee of the satellite and the associated slower speeds in those regions.

We examined data obtained over the interval from October 1, 1984 through October 31, 1985, during which time the satellite precessed slightly more than 24 hours in local time. No attempt was made to remove cyclical effects of solar origin although such effects are present. Figure 2 shows the daily average A_p index during the entire interval. This index, a measure of geomagnetic activity, is similar to the K_p index except that it is based on a linear scale as opposed to the

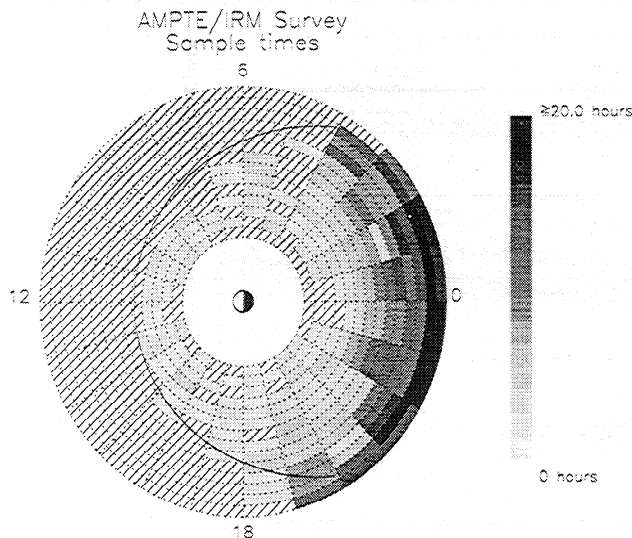


Figure 1. Observation times of AMPTE/IRM from October 1, 1984 through October 31, 1985. Cross-hatched bins represent those with less than 2 hours total time, which we require as a minimum for statistical purposes. Bins outside the magnetopause are typically cross hatched because of the requirement that the satellite be within the magnetopause, resulting in little or no observation time for these bins.

quasi-logarithmic scale of K_p . We first point out that the data used for this study were obtained at a time approaching solar minimum. The smoothed line shown in Figure 2 shows a clear decrease in A_p over the period although it can be seen that the change is small, implying that magnetic activity was relatively stationary for this period. The relevance of this information to occurrence rates presented in this work is difficult to quantify, although occurrence rates obtained during solar maximum would certainly be higher. Two other effects may be more important because they relate to changes in activity occurring over timescales shorter than the interval used in this study. The first is the 27 day solar rotation cycle, visible in the A_p index presented in Figure 2. Because the satellite's orbit precessed 0.95° per

day, relative peaks in occurrence rates should appear approximately every 26° , or 1.7 hours in magnetic local time. However, the bin size of 1 hour in local time results in spatial aliasing, so that the solar rotation peak is not visible in the plotted occurrence rates, although the effect is assumed to be present.

Finally, we also expect to observe seasonal variations [Bartels, 1963]. Such variations occur as a result of enhanced coupling between the solar wind and the Earth's magnetic field at vernal and autumnal equinoxes, and they account for increased activity at those times [Josselyn, 1995; Russell and McPherron, 1973]. From the smoothed line in Figure 2, however, it is apparent that this effect was not significant for our study. The reason may be related to the decreased activity associated with solar minimum.

3. Data Format and Analysis

This study was carried out by visually scanning plots of detrended magnetic field data and their dynamic spectra, as is shown in Figure 3. Durations of various events (defined below) were recorded as well as the satellite position during these times. Occurrence rates were calculated by normalizing the total event time by the total observation time for each L shell and hour in magnetic local time. The coordinate system, similar to that used by Anderson et al. [1990], is a spherical one with its polar axis aligned with the Earth's magnetic dipole and the data presented in radial (\mathbf{B}_R), eastward (\mathbf{B}_E), and compressional (\mathbf{B}_N) coordinates. In this system, compressional perturbations are directed along the background magnetic field, which is calculated from the observed field as described below; the background magnetic field so calculated is nominally northward. The eastward direction is taken to be the negative of the unit vector pointing from the center of the Earth in the direction of the satellite, crossed into the unit vector of the calculated background field. The radial direction is then calculated by crossing the eastward unit vector into the background field unit vector. Note that the radial

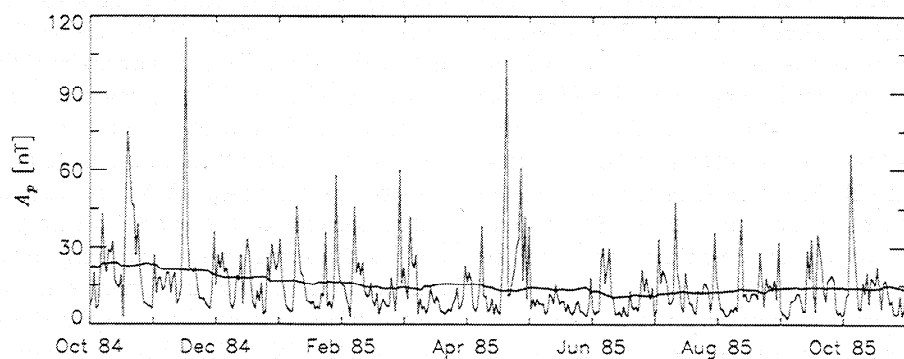


Figure 2. The daily average A_p index for the duration of this study. The smoothed line shows A_p averaged over 80 days and is an indication of the general trend. Although it shows a decrease in activity as solar minimum approaches, the change is small compared to normal activity.

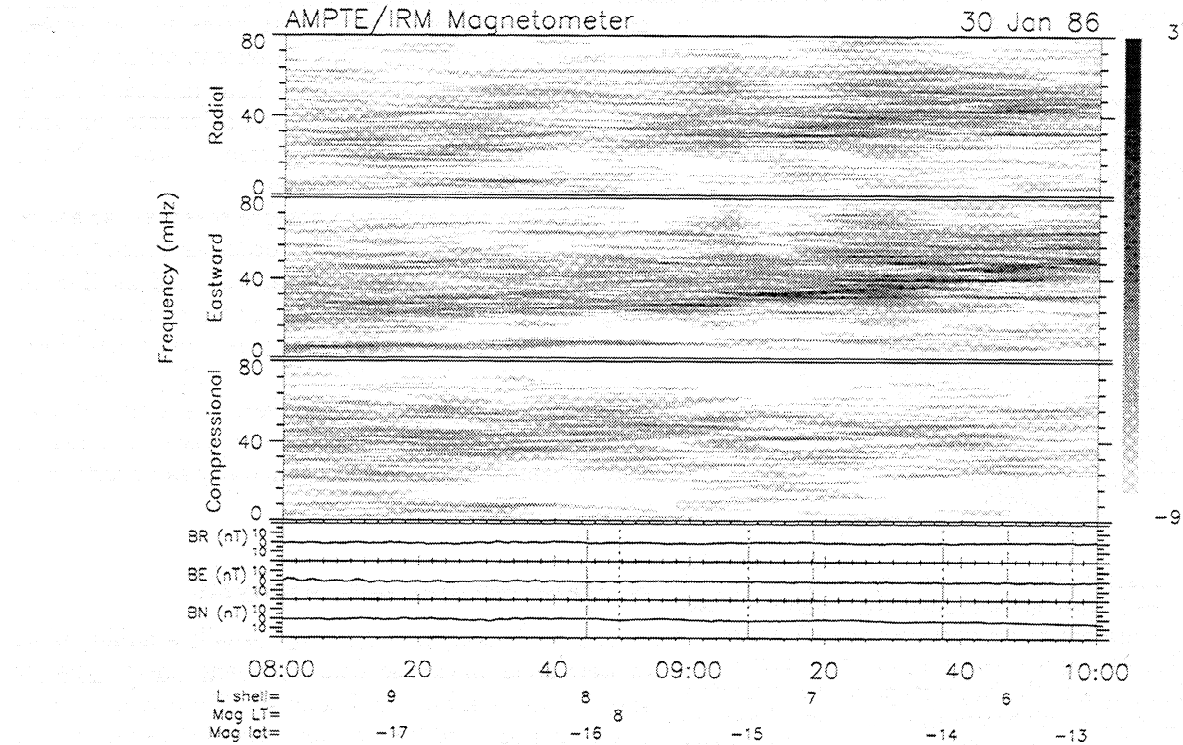


Figure 3. An example of the type of plot used in this study. The top three dynamic spectra are of the radial, eastward, and compressional components. The three detrended line plots at the bottom are of the same three components. Universal time is indicated along the horizontal axis, and vertical lines mark times when the satellite crossed into certain L shells or local times. This particular example shows the presence of a fundamental resonance of 3–10 mHz (from 0800 UT, fading at 0936 UT) and harmonic resonances ($f_{\text{peak}} > 10$ mHz) from 0820 UT through the end of the plot. Note the frequency dependence on L for both types of events.

direction does not strictly point outward from the center of the Earth because it depends on the orientation of the background field, which fluctuates constantly and is nominally dipolar, at least for the inner L shells. The data, while in a solar magnetic (SM) coordinate system, are then detrended by subtracting a background field, calculated point by point as follows [Zhu and Kivelson, 1991]. For each data point, a segment consisting of approximately 30 min worth of data (400 data points), whose midpoint occurs at the time of the data point, is fitted with a straight line. Segments of 30 min are used because they are effective in removing the background magnetic field without reducing $\text{Pc}5$ pulsation amplitudes. The value of the midpoint of the fitted line is taken to be the value of the background field at the time corresponding to the data point. The calculated background field is then used to calculate the compressional component $\mathbf{b} \cdot \mathbf{B}/B$, where \mathbf{B} is the background field and \mathbf{b} is the magnetic field data in the SM system. The other two components are calculated as described above.

Once data have been transformed to this system, dynamic spectra for each component are then calculated. No averaging is performed, and all of the data are used, retaining the sampling period of 4.5 s with a Nyquist frequency of 111 mHz. The data are whitened to reduce

background noise in the lower frequencies [Engelbreton et al., 1986], and then linear interpolation is used to fill gaps of 120 s or less. Segments of 256 points (approximately 19.2 min, resulting in a frequency resolution of 0.87 mHz) are then extracted and a Bartlett window is applied before calculating the fast Fourier transform. The window is advanced 60 s and the calculation is repeated until enough spectra have accumulated to fill 2 hour panels. Because of the large range in wave power in different regions such as the inner magnetosphere, the magnetosheath, and the solar wind, the power spectral density is plotted using a log scale that spans several orders of magnitude. With this scaling, the minimum detectable signal level is approximately 1 nT.

The satellite position is calculated assuming a dipole magnetic field. L shell, magnetic local time, and magnetic latitude information are included on the plots, although, as discussed above, latitudinal effects are ignored because of the sparse coverage. While a dipole field is appropriate for mapping regions in the inner magnetosphere, it is used here simply as a convenient means of organizing the data for the sake of comparison to AMPTE/CCE results of Anderson et al. [1990]. On the nightside, in particular, field line stretching will distort the field significantly from a dipole configuration, especially during active periods. Events occurring

at large L , especially on the nightside, probably do not realistically map to a footprint on the Earth calculated using the dipole mapping $r = L \cos^2 \theta$, where θ is invariant latitude.

4. Event Types and Sample Data

The main purpose for completing this survey is to identify regions within the magnetosphere where various types of pulsations tend to occur. Rather than selecting events solely on the basis of spectral and polarization characteristics, we have identified various types of events on the basis of a synthesis of properties reported in the literature. Naturally, certain types of pulsation events have been better identified than others. In cases where distinctions were not clear, we adopted a broader event definition than might be necessary in order to be confident that we included all events within a category. Our approach has a couple of consequences. First, it means that there are certainly times when activity is present but does not fit any of our event definitions. These intervals are ignored. Second, some of the definitions may be too broad and may unintentionally include pulsations excited by different and possibly unrelated sources. For these cases, while spatial occurrence distributions may provide useful information as to their sources, it is likely that more work is needed beyond this survey before they are well understood. In sections 4.1–4.4, we discuss each of the different types of events in detail.

4.1. Fundamental and Harmonic Resonances

Fundamental and harmonic resonances are probably the most easily observed and most well defined types of pulsations. The general idea is that standing waves are set up along magnetic field lines whose fundamental and harmonic frequencies depend inversely on the Alfvén transit time, which increases with higher L [Samson and Rostoker, 1972]. A satellite crossing field lines radially, then, observes oscillations in the azimuthal component of the magnetic field with a frequency that changes smoothly as a function of radial distance (while maintaining a coherent signal). Reports of observations of standing Alfvén waves by ATS 1 appeared nearly 30 years ago [Cummings et al., 1969]. Singer et al. [1982] later showed that electric and magnetic fields measured by ISEE 1 during these events were 90° out of phase, providing strong support for their standing nature. The harmonic structure has also been well studied and documented [Cummings et al., 1969; Engebretson et al., 1986; Takahashi and McPherron, 1982], and it now seems clear that satellites near $L = 5$ to $L = 9$ observe fundamental resonances below 10 mHz while harmonic resonances occur generally above 10 mHz. We emphasize that these resonances are associated with broadband excitation sources and not necessarily typical of field line resonances observed on the ground, which

most often appear to be present over some spatially thin region [Ruohoniemi et al., 1991; Walker et al., 1979].

For the purposes of this survey, we adopt definitions of fundamental and harmonic resonances identical to those used by Anderson et al. [1990]. Any resonance is first identified as a narrowband signal ($\Delta f \leq 10$ mHz) whose frequency decreases with increasing radial distance. The event is recorded as a fundamental resonance if its frequency is less than 10 mHz; otherwise it is recorded as a harmonic event. Anderson et al. [1990] were able to show that this definition was reliable by noting that the occurrence rate of fundamental mode resonances had a node near 0° magnetic latitude and that it increased smoothly with increasing latitude, consistent with the expected signature of an odd-mode resonance. We point out that consistent with the results of Takahashi and McPherron [1982] and Anderson et al. [1990], the presence of a fundamental resonance in our data did not seem to be necessarily well correlated with the presence of harmonics. Either type of event could appear independently of the other. Figure 3 shows a typical example of both types of resonances (visible as intensifications of power in the eastward component), occurring simultaneously in this case. The fundamental resonance begins at ~ 3 mHz and gradually approaches 10 mHz as it fades near 0936 UT. Harmonic resonances can be seen faintly as early as 0820 UT after which they intensify significantly. Note that although the signal levels in the detrended data are very low (fundamental resonances are often 15 nT or more), the dynamic spectra enhance these features significantly.

4.2. Storm Time Pulsations

Observations of magnetospheric fluctuations at $Pc5$ frequencies (1.7–6.7 mHz) with significant power in the compressional component of the magnetic field are very common. There are many types of phenomena that would have this signature, not all of which are pulsations. A partial list includes transient events [Borodkova et al., 1995; Sanny et al., 1996], sudden commencements [Kokubun, 1983], storm recovery phases [Baumjohann et al., 1987], dipolarization at substorm onset [Baumjohann et al., 1991], neutral sheet oscillations [Bauer et al., 1995], oscillations associated with substorm breakup [Holter et al., 1995], and $Pi3$ pulsations, possibly due to solar wind pressure fluctuations [Matsuoka et al., 1995]. Not included in this list are bursty bulk flows, which are discussed below.

Particular types of compressional signals commonly observed in the dayside and afternoon sectors have been well correlated with magnetic storms. Barfield et al. [1972], Barfield and McPherron [1972], Barfield and McPherron [1978], and Kokubun [1985] identified events that tend to be located in the afternoon sector and were able to associate them with substorms and the main phase of storms. Kremser et al. [1981] suggested that these pulsations may be associated with electron oscillations (of energy $E_e > 22$ keV) in phase with to-

tal magnetic field fluctuations and out of phase with ion oscillations (of energy $E_i > 27$ keV). In their work, *Barfield and McPherron* [1972] describe storm time pulsations as having a mean frequency of 5 mHz and a mean amplitude of 10 nT. Events typically last from 15 min to several hours, during which time the wave remains quasi-monochromatic with very nearly constant frequency. Events in their study ranged in frequency from 2.5 to 9 mHz, although 18 of the 20 events they studied had a frequency of 5 ± 2 mHz. *Barfield et al.* [1972] also mention that the compressional and radial components are, on average, in antiphase.

Higbie et al. [1982] and *Nagano and Araki* [1983] reported observations of compressional pulsations observed near magnetic noon, and they showed that they typically occur during the recovery phase of storms. These waves tend to persist for several hours (27 hours for the event reported by *Higbie et al.* [1982]) and have a maximum in frequency near local magnetic noon (at 13 mHz for one example) with lower frequencies on either side of noon. *Takahashi et al.* [1985] investigated eight events, including those first reported by *Higbie et al.* [1982] and *Nagano and Araki* [1983], although not all of the events were associated with the recovery phase of a storm. They determined that the azimuthal wave number for these events ranged from 40 to 120, that the waves typically propagated westward with a velocity of 10 km/s, and that harmonics of local standing Alfvén waves often occurred simultaneously. They were

also able to show that energetic electron flux oscillations remained in phase with energetic ion flux oscillations, both out of phase with fluctuations of the total magnetic field. *Kremser et al.* [1981] had also noted these characteristics of compressional pulsations near magnetic noon. Finally, *Takahashi et al.* [1985] note that the magnetic field signature typically shows a phase lag of 180° between the parallel and radial components and a phase lag of $\pm 90^\circ$ between the parallel and azimuthal components.

In their definition of storm time events, *Anderson et al.* [1990] included monochromatic pulsations ($\Delta f \leq 15$ mHz) if the upper frequency limit was 15 mHz or less and broadband pulsations ($15 \text{ mHz} \leq \Delta f \leq 80$ mHz) if the lower frequency limit was 5 mHz or less. In our definition of storm time pulsations we impose somewhat tighter constraints and require $\Delta f \leq 15$ mHz and $1 \text{ mHz} \leq f \leq 20$ mHz. We also require that the wave power in the northward and radial components be greater than that in the eastward component, similar to the constraint used by *Anderson et al.* [1990]. Using this definition, we expect to include both main phase and recovery phase related events as described above. We point out that it is not possible to distinguish between these two types of events on the basis of magnetic field data alone. Figure 4 shows the signature of a storm time pulsation along with high-frequency transverse pulsations. The high-frequency pulsations are different than harmonic resonances and are discussed in

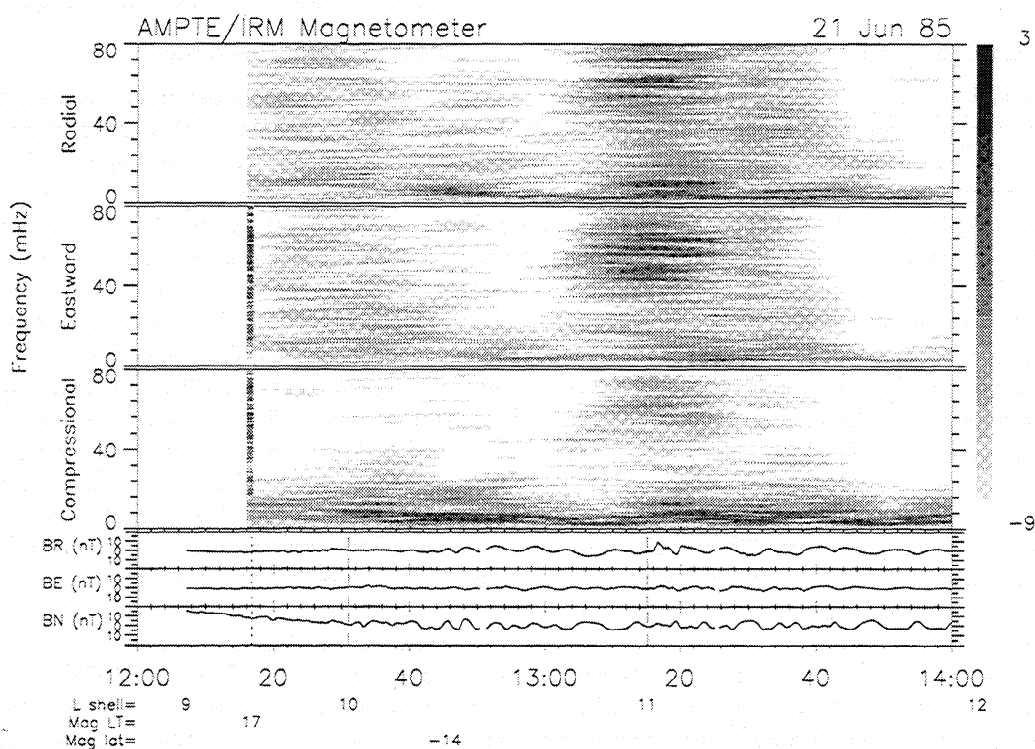


Figure 4. An example of storm time and related high-frequency transverse pulsations. Storm time activity can be seen from 1230 UT through the end of the plot. High-frequency transverse waves are visible only briefly in this example, near 1315 UT. Modest frequency doubling of the compressional component is present from 1240 to 1300 UT.

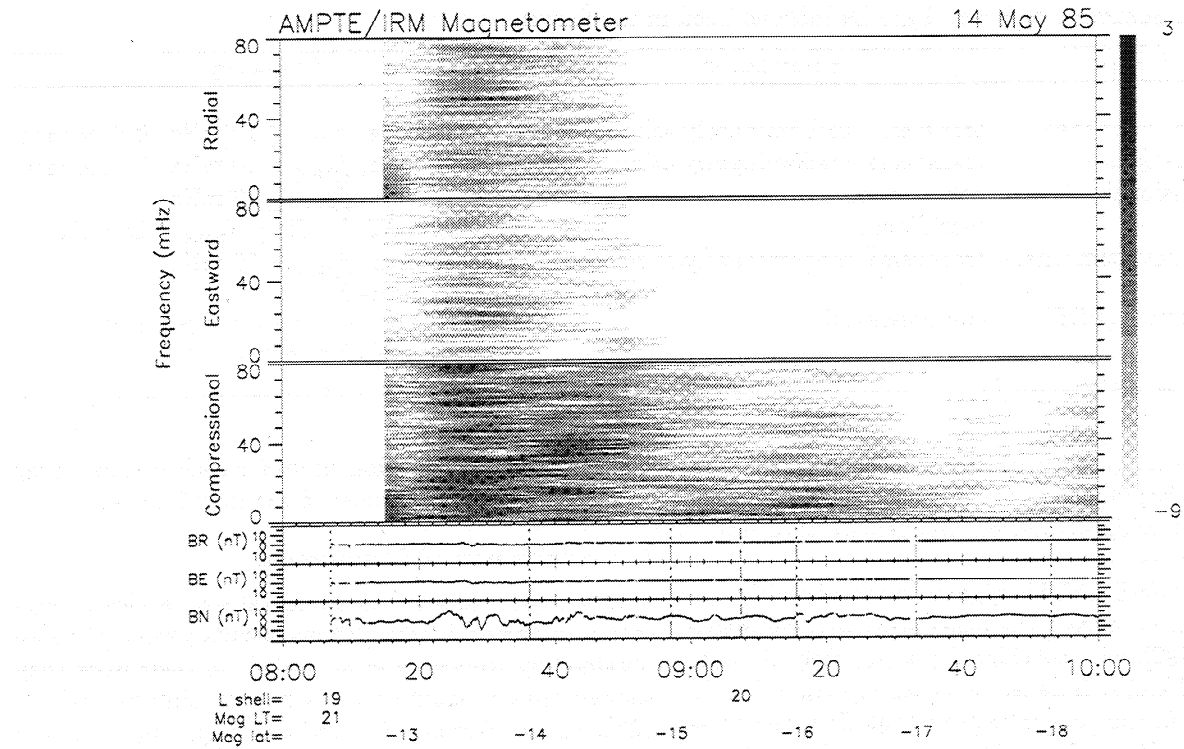


Figure 5. Magnetic signature of a bursty bulk flow. From the plasma data it was determined that the flow arrived at 0822:50 UT, although the signature in the magnetic field data is apparent beginning near 0821:10 UT. This event is typical in the sense that most of the power is present in the compressional component and the spectrum consists of discrete peaks superimposed on a broadband background.

section 4.3. Onset of the storm time pulsations occurs at 1230 UT and continues through the end of the plotted data. Note that the presence of frequency doubling of the compressional component occurs near 1300 UT. Frequency doubling of the compressional component of storm time pulsations was reported by *Coleman* [1970] and further investigated by *Higuchi et al.* [1986] and *Takahashi et al.* [1990a]. *Southwood and Kivelson* [1997] present a nonlinear theory explaining that such pulsations are associated with resonant ring current particles and that these waves play an important role in limiting ring current growth. *Higuchi et al.* [1986] called the type of activity in Figure 4 transitional because the compressional component contains power at the frequency of the radial component and twice that value. While the example in Figure 4 is not the clearest one in our data set, we omit frequency-doubling events from the survey because of the rarity of their occurrence. The low occurrence rate in our data set may be due to the restriction that the satellite must be within 2° of the magnetic equator to observe them [*Takahashi et al.*, 1990a].

4.3. High-Frequency Azimuthal Pulsations

High-frequency transverse pulsations such as those visible in Figure 4 at 1315 UT are observed occasionally by AMPTE/IRM. The duration of this particular event, ~ 10 min, is typical. We include events of this type in our survey because of their apparent associa-

tion with storm time pulsations. We require that they be transverse or azimuthally polarized, with frequencies such that $\Delta f \leq 10$ mHz and $f_{\text{peak}} \geq 20$ mHz.

4.4. Bursty Bulk Flows and Other Fast Flows

Angelopoulos et al. [1992] describe bursty bulk flows as intervals, typically lasting 10 min, in the inner central plasma sheet when plasma velocities are enhanced. Embedded within these intervals are brief “flow bursts” with velocities greater than 400 km/s lasting the order of 1 min. Flows are predominantly earthward and perpendicular to the background field. Of the events studied by *Angelopoulos et al.* [1992], 90% were associated with an AE index greater than 100 nT, and they suggest that these flow events may be important to plasma sheet transport during substorms if their cross section is the order of a few tens of R_E^2 . *Shiokawa et al.* [1998] recently analyzed one event in detail and showed that observation of a high-speed flow preceded formation of the current wedge by 3 min and geosynchronous particle injection by 6 min.

Figure 5 shows a typical magnetic signature of a flow burst, which was one of the events considered by *Angelopoulos et al.* [1992]. Although the flow arrives at 0822:50 UT (not shown), the signature in the magnetic field data is apparent near 0821:10 UT. As is typical for virtually all of the events studied, increased power is primarily present in the parallel (compressional) com-

Table 1. A Summary of Event Type Definitions Used in the Survey

Event Type	Polarization	Frequency
Fundamental resonance	transverse, predominantly azimuthal	$\Delta f \leq 10 \text{ mHz}$, $f_{\text{peak}} \leq 10 \text{ mHz}$, L dependent
Harmonic resonance	transverse, predominantly azimuthal	$\Delta f \leq 10 \text{ mHz}$, $f_{\text{peak}} > 10 \text{ mHz}$, L dependent
Pc3 compressional	compressional	$\Delta f \leq 10 \text{ mHz}$, $f_{\text{peak}} \geq 10 \text{ mHz}$
Storm time	meridional	$\Delta f \leq 10 \text{ mHz}$, $0 \text{ mHz} \leq f_{\text{peak}} \leq 20 \text{ mHz}$
High-frequency azimuthal	transverse, predominantly azimuthal	$\Delta f \leq 10 \text{ mHz}$, $f_{\text{peak}} > 10 \text{ mHz}$, L independent
Bursty bulk flow (BBF)	compressional	broadband with discrete peaks, maximum duration of 30 minutes

ponent of the magnetic field with a spectrum consisting of increased broadband noise accompanied with peaks in power occurring at discrete frequencies throughout the 0-80 mHz range.

We include events of this type in our survey, although the definition is relaxed from that used by Angelopoulos *et al.* [1992], who considered plasma sheet flows in excess of 400 km/s. Because we consider magnetic field data alone, we no longer require that flow velocities exceed 400 km/s, and we place no restrictions regarding the location of the satellite. We only require that a flow event has a signature as described above. In particular, we require that (1) the power be primarily compressional, (2) the spectrum have a low-level broadband background, (3) peaks appear in the spectrum at discrete frequencies, and (4) the event duration be less than 30 min. The last constraint is imposed in order to exclude compressional activity associated with substorms that does not result from the passage of a bursty bulk flow. Such activity might result from substorm dipolarization, fast mode waves excited in conjunction with substorm onset, or other types of phenomena that are not yet well understood. By using a relaxed event definition for this survey, our intention is to consider all flow-type events in any region, not just plasma sheet flows with speeds greater than 400 km/s. Angelopoulos *et al.* [1994] investigated the occurrence distribution of bursty bulk flows, noted a decreased occurrence rate nearer the Earth, and suggested that flow speeds decrease as bursty bulk flows approach the Earth. By relaxing the constraint that flow speeds exceed 400 km/s, we hope to determine occurrence distributions of the flows as they decelerate. Finally, we point out that fast flows are typically embedded in bursty bulk flows and do not appear separately in our study.

5. Results

Table 1 shows a summary of the event definitions described in section 4. For each event type, the survey was completed by examining both line plots and dynamic spectra, plotted as shown in Figures 3, 4, and 5, and recording total observation time along with event times. Occurrence rates are calculated by dividing event

times by total observation times for each bin, and they are presented and discussed in sections 5.1-5.4.

5.1. Fundamental Resonances

Occurrence rates for fundamental resonances are presented in Figure 6, which shows results similar to those obtained by Anderson *et al.* [1990]. In their work they showed that fundamental resonances observed within 13° of the equator are observed less frequently (less than 40%) than those observed at higher latitudes are (nearly 80%), and they attribute this difference to the presence of a node near the equator because of the odd mode resonance. As mentioned in section 2, AMPTE/IRM sampled $\pm 40^\circ$ in magnetic latitude, which when combined with the relatively fast speed of the satellite, resulted in poor statistical coverage as a function of latitude. For this reason, we ignore latitudinal effects and present only the occurrence rates observed for all latitudes, obtaining a maximum rate of 57%, consistent with the results of Anderson *et al.* [1990].

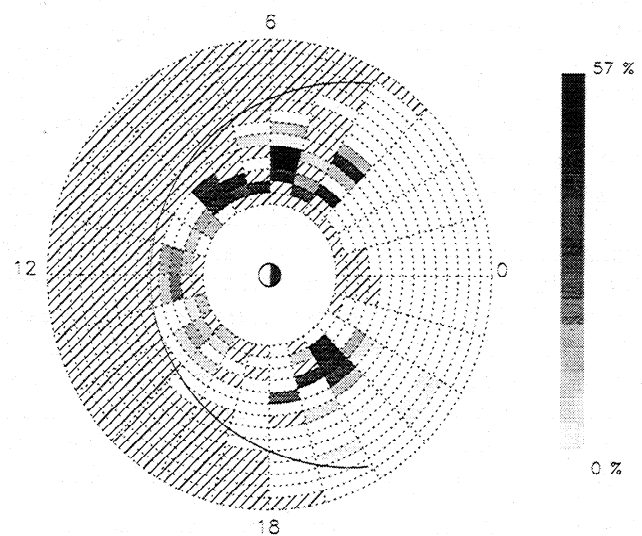


Figure 6. The occurrence distribution of fundamental field line resonances. Note the pronounced dawn-dusk asymmetry in occurrences. Also, note the lack of resonances near the magnetopause, likely an indication that the source spectrum does not contain power below a certain frequency, which we estimate to be $\sim 10 \text{ mHz}$.

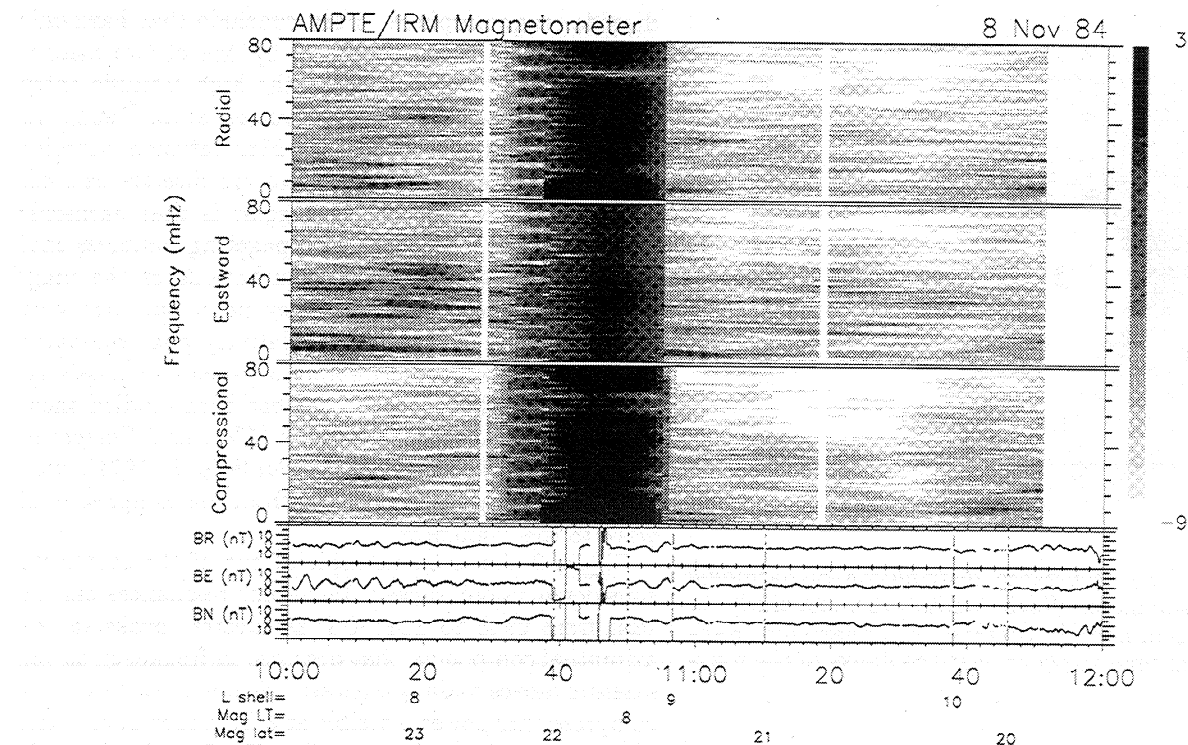


Figure 7. An example of how the signature of a fundamental resonance fades as the satellite approaches the magnetopause. The resonance appears at 1000 UT as a narrow banded structure near 7 mHz in the eastward component only. The signal fades near 1040 UT but intensifies somewhat and then fades finally at ~ 1112 UT after its frequency has decreased to ~ 3 mHz. Note that the signal fades near $L = \sim 9.2$ but that the satellite does not encounter the magnetosheath until near $L = \sim 10.2$.

Perhaps the most useful information in Figure 6 is concerned with the spatial aspects of the occurrence rates. In spite of the poor sampling of some regions, it seems clear that fundamental resonances are not typically observed near the magnetopause. Although it may be suggested that the field topology and motion of the magnetopause may have shielded their signature, we note that we found no cases where a fundamental resonance was observed as the satellite encountered the magnetopause. Figure 7 shows an example of how the signal of a fundamental resonance fades near the magnetopause. The resonance appears in Figure 7 (at 1000 UT) as a narrow banded structure near 7 mHz in the eastward component only. As the satellite crosses field lines (moving radially outward), its frequency decreases to a minimum near ~ 3 mHz. The signal can be seen to fade initially near 1040 UT (in spite of the bad data segment) but intensifies somewhat and then fades for the last time at ~ 1112 UT in the region of $L = \sim 9.2$. Magnetic fluctuations typical of the magnetosheath begin to appear at 1150 UT, when the satellite is close to $L = \sim 10.2$.

A similar trait can be noted regarding the high-frequency end of fundamental resonances. Figure 3 shows an example of how the frequency of a fundamental resonance typically appears to not exceed 10 mHz. The signal, nominally ~ 3 mHz at 0800 UT, increases

to ~ 10 mHz as the satellite moves radially inward before fading near $L = \sim 6.4$ at 0936 UT. This behavior, combined with the fact that harmonic resonances are not strongly associated with fundamental resonances and the discussion of the previous paragraph, suggests that the excitation source is band limited. We conclude that the excitation source must contain power at frequencies ranging from ~ 3 to 10 mHz. A Kelvin-Helmholtz instability acting at the magnetopause has often been invoked as the excitation source of field line resonances. Miura [1987] modeled this instability at the magnetopause and predicted that perturbations should occur in the frequency range from 3.2 to 9.3 mHz, which is consistent with our results. This lends strong credibility to the association of fundamental resonances with the Kelvin-Helmholtz instability.

Although it is apparent from Figure 6 that fundamental resonances can be detected over a very broad range in local time, Figure 6 also shows that they are most likely to occur near dawn, a result consistent with that of other studies [Anderson *et al.*, 1990; Kokubun, 1985; Kokubun *et al.*, 1989; Takahashi and McPherron, 1984]. Assuming that a Kelvin-Helmholtz instability is responsible for fundamental resonances, it may seem that occurrence rates at dawn and dusk should be similar. Anderson *et al.* [1990] considered the possibility that fundamental resonances on the dusk side are

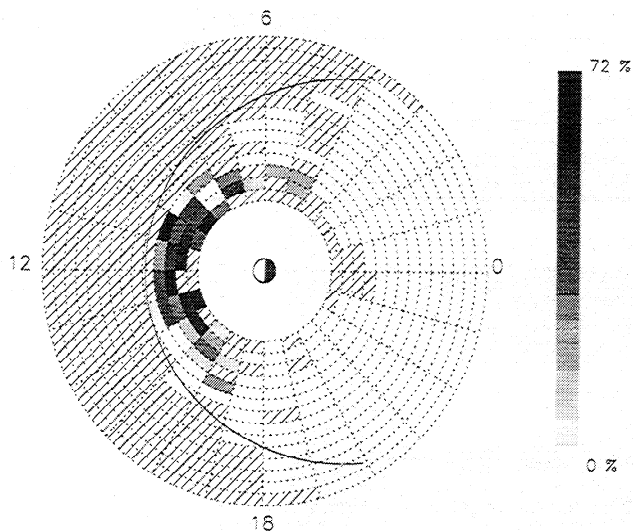


Figure 8. The occurrence distribution of harmonic field line resonances. Such events are most likely to occur near local noon in contrast to fundamental resonances, which tend to occur near the flanks of the magnetosphere.

present but are masked by other pulsation activity, although their result was inconclusive. However, results from the model of *Lee et al.* [1981] show that the instability criterion is more easily satisfied in the morning sector, which may explain the reason for the dawn-dusk asymmetry noted in the various studies. In particular, excitation of the magnetopause in their model depends on the magnitude and direction of the magnetosheath magnetic field. Because the magnetosheath magnetic field intensity in the morning sector is generally smaller than that in the afternoon, the instability criterion for the instability is more easily satisfied in the morning sector.

5.2. Harmonic Resonances

Occurrence rates of harmonic resonances are presented in Figure 8. The spatial distribution is again similar to that of *Anderson et al.* [1990], except that the peak in our survey occurs near noon, while theirs occurs a few hours earlier. The reason for the discrepancy is not clear, although it may be due to the difference in latitudes sampled by the satellites. The maximum occurrence rate that they obtain, near 63%, is similar to ours of 72%.

The relatively uniform occurrence distribution as a function of radial distance is noted by *Anderson et al.* [1990] and may well have implications regarding the excitation source for these resonances. In particular, such a distribution implies that the source permeates the dayside magnetosphere uniformly. *Anderson and Engebretson* [1995] compared the relative power of all three components of magnetic field data obtained by AMPTE/CCE in an attempt to determine the source of harmonic and broadband resonances observed in the

dayside magnetosphere. They conclude that harmonic resonances are likely generated by one of two mechanisms. The first possibility is the high-latitude entry mechanism discussed by *Engebretson et al.* [1991]. In this case, coupling occurs at the high-latitude footprint of the field line where resonances are directly excited. The second possibility they suggest is that harmonic resonances are generated by propagating compressional oscillations resulting from perturbations of the magnetospheric cavity, although they point out that such a cavity would have to be a relatively poor resonator (its Q would be low). Coupling between compressional waves and field line resonances has been studied theoretically by a number of authors [*Chen and Hasegawa*, 1974; *Hasegawa et al.*, 1983; *Southwood*, 1974], who show that energy is transferred from the compressional wave to the resonance.

Figure 9 shows an example of one of the events we considered in our survey. Harmonic resonances can be seen from 0945 to 1147 UT as spectral peaks in the azimuthal component that decrease in frequency as the satellite moves radially outward. Beginning at 0922 UT, compressional power is visible at a frequency of 31 mHz, which gradually decreases to 24 mHz. Low-level broadband compressional power is also seen throughout the interval from ~ 20 to 60 mHz. Although we have not investigated this event in detail, it seems likely that the narrowband compressional power plays a significant role in the excitation of the harmonics, given its greater intensity relative to the broadband compressional power. At 1048 UT (near $L = 7.6$) the azimuthal power intensifies as the compressional power subsides, suggesting that the two modes are coupled at this point and that energy is transferred to the harmonic mode, although it can not be determined with certainty from Figure 9 whether this effect is entirely spatial or temporal. This event, along with at least a few others like it, prompted us to include narrowbanded compressional pulsations with frequencies greater than 10 mHz in our study. Figure 10 shows the spatial occurrence distribution of these events, and it is immediately clear that they are observed in regions that overlap with observations of dayside harmonic events, a result consistent with a study by *Yumoto and Saito* [1983]. *Takahashi and Anderson* [1992] used data from AMPTE/CCE and showed a peak in $Pc3$ compressional power from $L = 3$ to $L = 5$ in the prenoon region. However, they also showed that at least at 10 mHz (see their Plate 4), an additional peak was observed postnoon for $L > 5$, consistent with our results, although we only consider narrowband signatures while they had no such restriction. They suggest that these waves may result from coupling to toroidal resonances observed in the region or, alternatively, that compressional power originates from interactions of the solar wind with the magnetopause and subsequently propagates earthward. Our results presented in Figure 10 show an increased probability of occurrence of these waves in the outer L shells (up to

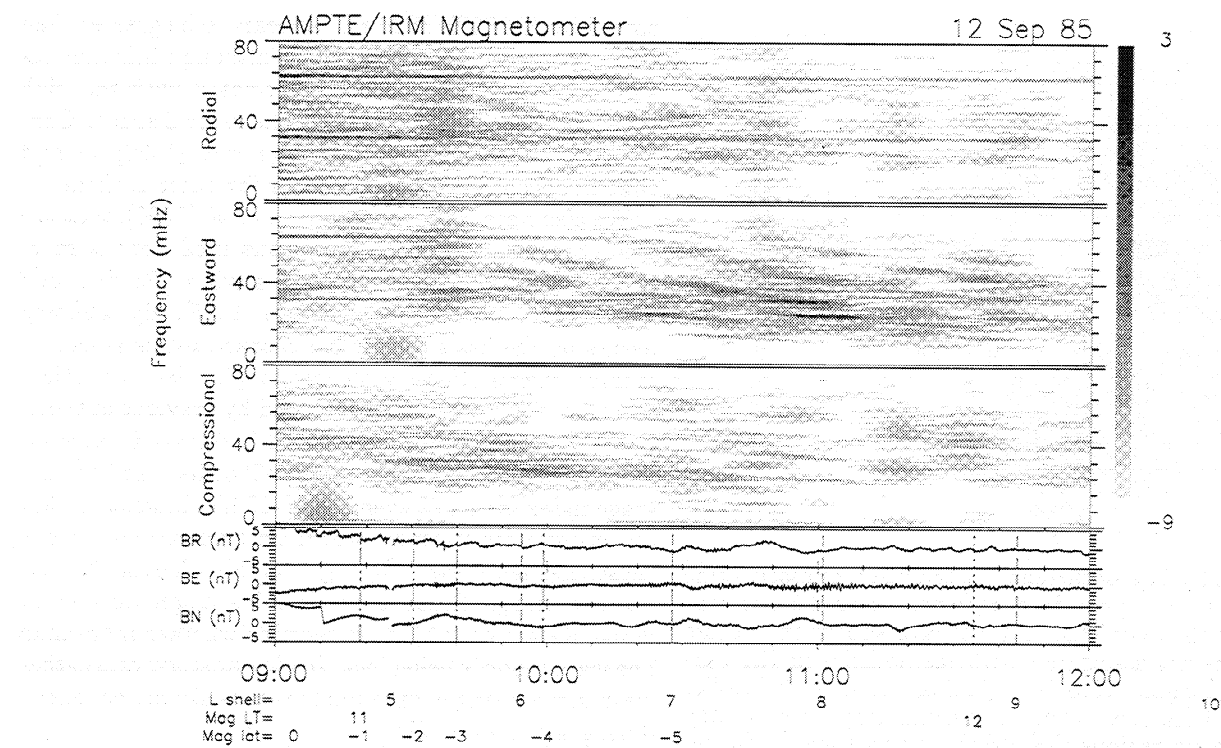


Figure 9. An example showing the simultaneous occurrence of harmonic resonances and compressional $Pc3$ pulsations. Harmonic resonances, visible in the eastward component, are present from 0945 to 1147 UT. The compressional signature begins at 0922 UT at a frequency of 31 mHz and decreases to 24 mHz as it fades near 1050 UT. The disappearance of the compressional signature at nearly the same time as the enhancement of the harmonic resonance suggests coupling of the two modes and energy transfer to the harmonic mode.

the magnetopause), suggesting that the latter situation is more likely.

The occurrence of compressional pulsations in the same region where harmonic resonances are observed

suggests that the resonances are likely excited by the compressional pulsations in at least some cases. *Anderson and Engebretson [1995]* pointed out that in order for this coupling to occur, both modes should be observed simultaneously, basically in agreement with the example shown in Figure 9. On one hand, our results indicate that harmonic resonances are excited by compressional oscillations. However, the peak occurrence rate of the resonances (72%) is significantly greater than the peak occurrence rate of the compressional waves (27%). Unless this discrepancy is due to some unknown latitudinal effect, it appears that harmonic resonances on the dayside may also be excited via the high latitude mechanism described by *Engebretson et al. [1991]*.

5.3. Storm Time and High-Frequency Azimuthally Polarized Pulsations

Figure 11 shows occurrence rates of storm time pulsations. It is apparent from Figure 11 that storm time pulsations can be detected at almost any location within the magnetosphere. We should point out that occurrence rates (near dusk) that lie outside the average magnetopause position drawn on the plot are actually within the magnetosphere, although the occurrence distribution suggests that these pulsations can occur very close to the magnetopause. Consistent with the results

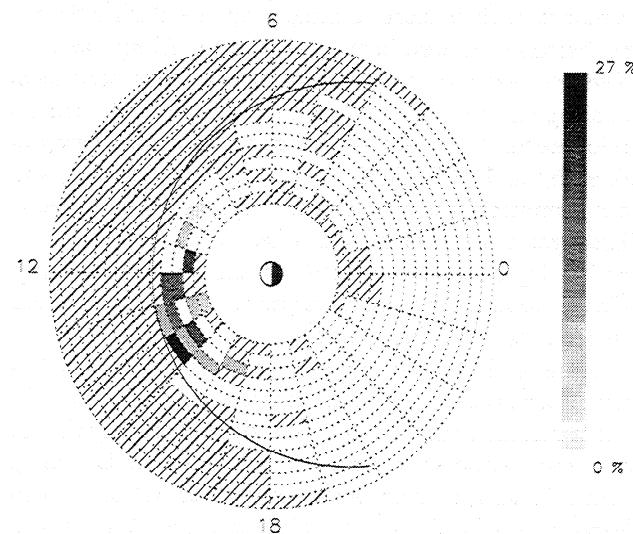


Figure 10. The occurrence distribution of $Pc3$ compressional pulsations. The peak in occurrences just after local noon overlaps the region where harmonic resonances are also observed.

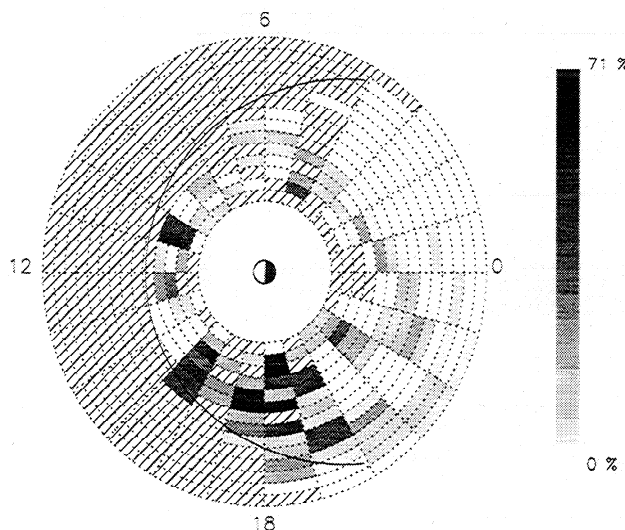


Figure 11. The occurrence distribution of storm time pulsations. The peak in occurrences near dusk is consistent with other studies that have shown that these pulsations are associated with instabilities in the partial ring current. The distribution shown here implies that particles that form the partial ring current may be present in regions close to the magnetopause during storms and substorms.

shown in Figure 11, *Anderson et al.* [1990] showed that the occurrence rate of storm time pulsations is significantly greater for outer L shells. Using AMPTE/CCE data, they reported that events occur less than half as often in the $L = 6-7$ region as they do in the $L = 8-9$ region. Our observations show a peak in the occurrence rate of storm time pulsations between $L = 10$ and $L = 12$.

Kremser et al. [1981] identified spatial distributions of storm time events using data from GEOS 2 at geosynchronous orbit. They noted two peaks in their distribution, one at dusk and another near noon with approximately twice the occurrence rate. Our data, which are not of geosynchronous origin, show a clear peak near dusk and a very modest peak near noon, similar to the results of *Zhu and Kivelson* [1991], who used ISEE 1 and 2 data but also observed events on the dawn side. We point out, however, that they considered compressional events in general, with a more relaxed definition than ours. Our results are also similar to that of *Anderson et al.* [1990], with a couple of notable exceptions. First, their work shows a clear peak in the predawn hours while ours does not. Figure 11 does show a slightly increased probability that events will occur in the predawn region, but a clear peak is not visible. Second, our maximum occurrence rate of 71% is significantly higher than theirs, which is $\sim 50\%$ when AMPTE/CCE was within 4° of the equator. However, we note that the maximum occurrence rate in our data set occurred beyond the region where AMPTE/CCE was able to sample. In the regions where AMPTE/IRM and AMPTE/CCE observations overlap, the rate ob-

served by AMPTE/IRM still appears to be greater than that observed by AMPTE/CCE, although this may result from the poor statistics associated with the high speed of AMPTE/IRM through the inner L shells. Consistent with the study of *Anderson et al.* [1990], we find that the occurrence rate is higher for outer L shells.

We also note, as does *Anderson et al.* [1990], that the definition of storm time pulsations used here is more general than that used in early studies [*Barfield and McPherron*, 1972, 1978; *Kokubun*, 1985]. By selecting events on the basis of spectral characteristics alone, we include events (those with low amplitudes in particular) that would have been excluded by previous authors. Only half of the 95 events selected in our study were associated with a D_{st} index of -10 nT or less, and the average index for all 95 events was -15 nT, indicating that our criteria for selecting storm time pulsations include those that are present during intervals when storms are not occurring. Because we examine magnetic spectra alone, we are not able to determine whether more than one wave mode is being included in our study or whether we observe a single wave mode that is simply enhanced during storm intervals.

Kremser et al. [1981] were able to show that events contributing to peaks in occurrence distributions at noon and dusk are likely generated by a drift mirror instability, associated with a high β plasma [*Hasegawa*, 1975; *Lanzerotti et al.*, 1969]. *Barfield and McPherron* [1972] showed a strong correlation between events near dusk and substorms, and they suggested that the pulsations may be associated with a peak in the partial ring current. If storm time pulsations are excited via ring current particle populations, as was strongly suggested by the various studies, then Figure 11 may provide some information as to the spatial distribution of injected particles. In particular, Figure 11 implies that particles that form the partial ring current may be present in regions close to magnetopause during storms or substorms, at least in the dusk sector. *Hamilton et al.* [1988] showed that ring current populations near local noon can show enhanced densities out to $L = 8$ during a major storm. The data they showed, however, were obtained by AMPTE/CCE (with apogee of $8.8 R_E$), and no information was available for regions beyond $L = 8$. *Takahashi et al.* [1990b] and *Wodnicka* [1989] modeled particle injections during storms and showed that significant populations can be present out to $L = 10$ and greater in the the dusk sector.

Figure 4 shows the presence of relatively high frequency transverse pulsations centered around 1315 UT. The transient character of these signals is typical, and their association with storm time pulsations is strong. Figure 12 shows their occurrence distribution, which clearly peaks in the same region as storm time pulsations. While not all storm time events included high-frequency transverse signals, 72% of the high-frequency events we considered occurred at the same time as storm time pulsations, and all of the high-frequency events

at local times greater than 1600 magnetic local time (MLT) occurred when storm time pulsations were also present. In all cases, the high-frequency signal is transverse and in the frequency range typical of ion cyclotron waves. The event shown in Figure 4 with frequencies ranging from 40 to 70 mHz is common. André [1985] discusses electromagnetic and electrostatic waves in this frequency regime and presents dispersion surfaces for a number of models, including the case with three ion components, protons and singly ionized helium and oxygen. He shows that helium cyclotron waves can exist at frequencies below the helium cyclotron frequency if oxygen is present, which is often the case during magnetic storms. The helium cyclotron frequency for the example in Figure 4 is estimated to be ~ 115 mHz, on the basis of a dipole magnetic field. The dispersion surface presented in Figure 6 of André [1985] shows the frequency dependence on k_{\parallel} for various waves, and it indicates that the 40 to 70 mHz fluctuations are likely to be helium cyclotron waves, i.e., waves on the helium cyclotron dispersion surface (left-hand polarized) for parallel propagation, which asymptotically approaches the helium cyclotron frequency for large k_{\parallel} . Such waves may be associated with compressional perturbations that induce a temperature anisotropy, which is ultimately responsible for wave growth. While the occurrence of cyclotron waves during low-frequency compressional wave activity suggests that the Pc5 waves may play a role in the excitation of the cyclotron waves, more work needs to be done before this can be verified.

5.4. Bursty Bulk Flows and Other Fast Flows

The occurrence rate distribution of events associated with fast flows is presented in Figure 13. Occurrence

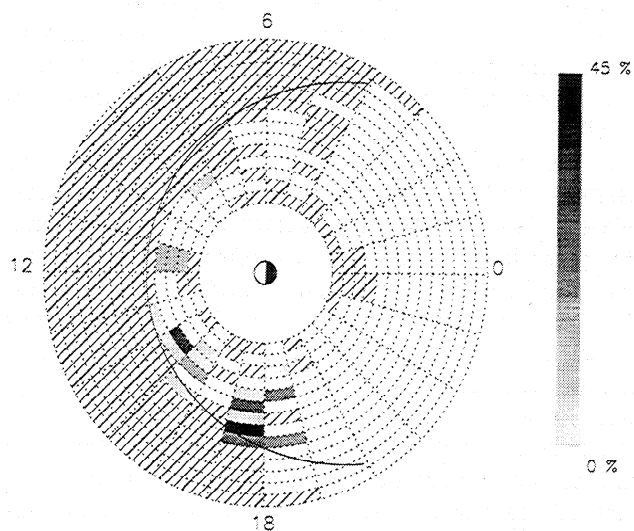


Figure 12. The occurrence distribution of high-frequency transverse pulsations. We show an association of these waves with storm time pulsations in the text. This distribution shows that occurrences are located in the same region as that where the peak in storm time pulsations occurs.

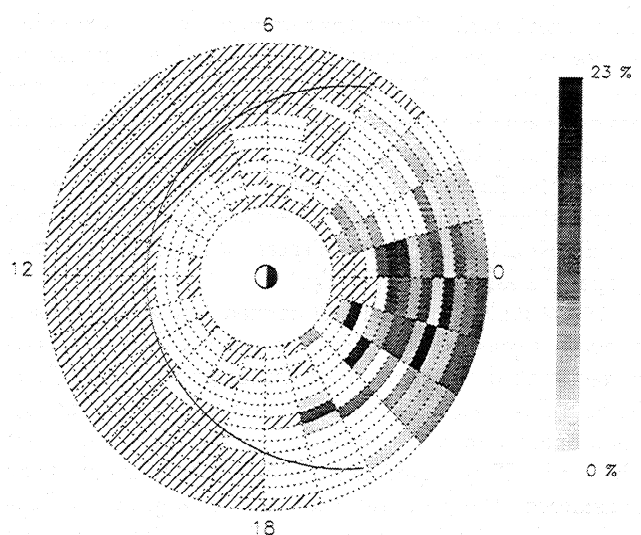


Figure 13. The occurrence distribution of bursty bulk flows and other fast flows. The distribution is similar to that shown by Angelopoulos et al. [1994] except that our occurrence rates are more uniform across L shells, which probably results from our more general event definition. By not requiring that flows have a minimum speed, our data show a relatively higher occurrence rate than that shown by Angelopoulos et al. near the Earth. We also note that the occurrence distribution suggests that flows propagate radially.

rates of fast flows have been investigated by a few authors [Angelopoulos et al., 1994; Baumjohann et al., 1990; Shiokawa et al., 1997], all of which used plasma data. While we completed our survey using only magnetic field data and note that we may have included events other than fast flows, the results we obtained have an occurrence distribution similar to these other studies. We note that our criteria for selecting these events resulted in the inclusion of all of the events reported by Angelopoulos et al. [1994], although others were included as well.

The most important feature in Figure 13 is the increased probability of occurrence in the premidnight region, lending support to the association of fast flows with substorms. This pattern is similar to that of Angelopoulos et al. [1994], and we arrive at similar occurrence rates, which is somewhat unexpected given that we do not require the minimum flow speed to be 400 km/s in our event definition as they do. In addition, each of the above studies finds that occurrence rates of fast flows are higher for more distant regions, out to 19 R_E . On the other hand, our results seem to show occurrence rates fairly uniformly distributed with respect to radial distance. Because we consider magnetic field data alone, it may be the case that we have included events in our survey that were not "flow" events, although we expect that this number would be small. If this is the case, the difference between our occurrence distribution and that of Angelopoulos et al. [1994] may indicate that flow speeds tend to decrease as the flows

move earthward, since Angelopoulos et al. excluded events with speeds below 400 km/s and we impose no such restriction. *Shiokawa et al.* [1997], on the other hand, determined that bursty bulk flows in the central plasma sheet are stopped rather abruptly as they approach the Earth, and the debate of how flows are decelerated continues. Finally, we note that the shape of the distribution pattern in Figure 13 implies that flows propagate earthward radially.

Angelopoulos et al. [1992] carried out a superposed epoch analysis to show that bursty bulk flows are associated with dipolarization of the magnetic field. That is, as a flow passes the satellite, an increase in the B_Z component and a decrease in the B_X component are observed. They noted that in 50% of the events they considered, the field returned to its original configuration after the flow passed, while for the remaining events the field remained dipolar afterwards, implying a possible relation to substorm dipolarization. The signature of a typical flow burst, presented in Figure 5, shows that most of the power in the magnetic field fluctuations occurs in the compressional component. This is reasonable if we consider the following. In the case where the flow is perpendicular to the background field, magnetic field lines will be forced to be compressed in front of the peak in the flow, resulting in a smooth increase in the parallel component of the magnetic field. The increased parallel component will appear as a dipolarization regardless of the behavior of the radial component because the elevation angle will change by virtue of the increased parallel component alone. In the case of oblique crossings of the background field, power will appear in the transverse components as well, and this is often observed in our data set. *Baumjohann et al.* [1990] showed that nearly all flows in the outer central plasma sheet and plasma sheet boundary layer are primarily field aligned but that 60-70% of the flows in the neutral sheet are mostly perpendicular. Of the events considered by Angelopoulos et al., most were perpendicular to the background field. While the scenario described here can explain the magnetic field signature of fast flows, the dipolarization associated with it would be transient and so would not support the idea that fast flows are directly responsible for substorm dipolarization.

Finally, we note that the discrete peaks in the compressional component visible in Figure 5 are present with virtually every flow burst. Inspection of ~ 20 events seems to show that at least for a few cases, these peaks result from a transient (but distinct) decrease in the compressional component of the field. In the same way that Fourier decomposition of a square wave shows power in the odd harmonics only, a transient decrease might be expected to have a discrete spectrum.

6. Discussion and Conclusions

Magnetic field data from the AMPTE/IRM satellite were used to complete a survey of occurrence rates of

a number of different types of pulsations. The satellite apogee of $\sim 18.8 R_E$ has allowed the outer regions of the magnetosphere to be included in the survey, although we have taken care not to include magnetosheath or solar wind data. Because of inadequate sampling of magnetic latitude (which spanned $\pm 40^\circ$), occurrence rates are projected into the equatorial plane, where they are binned according to L shell and magnetic local time. The total observation time of 1148 hours resulted in reasonable statistics, although a large portion of this time was concentrated at higher L values because of the highly elliptical trajectory of the satellite.

A number of different types of pulsations were included in the survey. Except for fluctuations associated with bursty bulk flows and other fast flows, event types were defined on the basis of a synthesis of descriptions reported in the literature. Using these definitions, occurrence rates were determined by inspecting 2 hour panels of dynamic spectra and detrended line plots. The following paragraphs summarize our most important conclusions.

1. Fundamental resonances were observed to occur over a limited range of L shells. In particular, we found that they tended to be absent from regions within 1 or $2 R_E$ of the magnetopause in the dawn sector, where they are observed most often. There is no obvious reason for this confinement in L unless it is an indication of the spectral content of the source. On the basis of this argument, we place a lower limit on the excitation source of fundamental resonances at ~ 3 mHz.

We also note that harmonic resonances are not well correlated with fundamental resonances. Again, this implies that the source of fundamental resonances must be band limited, and we place an upper frequency limit on the source spectrum of ~ 10 mHz. These frequency limits are virtually identical to the results of *Miura* [1987], who modeled a Kelvin-Helmholtz instability at the magnetopause, lending strong support to the idea that fundamental resonances are excited by such an instability.

2. We have found, consistent with other studies, that harmonic and fundamental resonances are not well correlated. However, we have shown that compressional Pc3 pulsations are observed just after local noon, a region that includes observations of harmonic resonances. We have also shown an example of the simultaneous occurrence of Pc3 pulsations and harmonic resonances, and we conclude that at least some of the harmonic events that occur later than noon are likely excited by compressional Pc3 pulsations. However, the occurrence rate of the compressional pulsations is less than half that of the resonances, so it appears that the resonances may also be excited by other means, perhaps the high-latitude entry mechanism described by *Engelbreton et al.* [1991].

3. On the basis of the spatial distribution of storm time pulsations, our results suggest that particles that form the partial ring current may extend to the magne-

topause during storms and substorms. Storm time pulsations, associated with the partial ring current and believed to result from a drift mirror instability of ring current particles [Barfield and McPherron, 1972; Kremser et al., 1981], are observed at L shells that are very close in proximity to the magnetopause in the dusk region.

We have also shown high-frequency transverse waves ranging from 40 to 70 mHz occurring simultaneously with storm time pulsations. The high-frequency waves appear to be helium cyclotron waves whose frequency indicates the presence of oxygen. Such waves are often excited by magnetic field compressions that cause a temperature anisotropy, which is ultimately responsible for wave growth. This scenario suggests that the compressional signature of storm time pulsations may play a role in their excitation, although a more thorough analysis needs to be done.

4. We have shown that the magnetic field signature of bursty bulk flows and other fast flows is compressional in nature. Flows that move perpendicular to a background magnetic field will necessarily compress the field lines in front of the flow, which could be responsible for the observations presented above. Such a process would imply that the dipolarization observed with the passage of a fast flow is transient and would not contribute to dipolarization commonly associated with substorms.

We have also noted the presence of discrete peaks in the spectrum of the compressional component. Inspection of a number of events seems to show that these peaks may result from Fourier analysis of a transient decrease in the compressional component of the field, although a more detailed analysis is warranted.

Acknowledgments. We acknowledge a number of useful discussions with B. J. Anderson, V. Angelopoulos, R. E. Denton, S. Elkington, J. LaBelle, W. Lotko, A. Miura, and R. Treumann. This research was supported at Dartmouth College by NASA grants NAG 5-2252, NAG 5-1098, and NGT 5-500059.

Janet G. Luhmann thanks Hitoshi Matsuoka and another referee for their assistance in evaluating this paper.

References

- Anderson, B. J., and M. J. Engebretson, Relative intensity of toroidal and compressional Pc 3-4 wave power in the dayside outer magnetosphere, *J. Geophys. Res.*, **100**, 9591, 1995.
- Anderson, B. J., M. J. Engebretson, S. P. Rounds, L. J. Zanetti, and T. A. Potemra, A statistical study of Pc 3-5 pulsations observed by the AMPTE/CCE magnetic fields experiment, 1, Occurrence distributions, *J. Geophys. Res.*, **95**, 10,495, 1990.
- André, M., Dispersion surfaces, *J. Plasma Phys.*, **33**, 1, 1985.
- Angelopoulos, V., W. Baumjohann, C. F. Kennel, F. V. Coroniti, M. G. Kivelson, R. Pellat, R. J. Walker, H. Lühr, and G. Paschmann, Bursty bulk flows in the inner central plasma sheet, *J. Geophys. Res.*, **97**, 4027, 1992.
- Angelopoulos, V., C. F. Kennel, F. V. Coroniti, R. Pellat, M. G. Kivelson, R. J. Walker, C. T. Russell, W. Baumjohann, W. C. Feldman and J. T. Gosling, Statistical characteristics of bursty bulk flow events, *J. Geophys. Res.*, **99**, 21,257, 1994.
- Barfield, J. N., and R. L. McPherron, Statistical characteristics of storm-associated Pc 5 micropulsations observed at the synchronous equatorial orbit, *J. Geophys. Res.*, **77**, 4720, 1972.
- Barfield, J. N., and R. L. McPherron, Stormtime Pc 5 magnetic pulsations observed at synchronous orbit and their correlation with partial ring current, *J. Geophys. Res.*, **83**, 739, 1978.
- Barfield, J. N., R. L. McPherron, P. J. Coleman Jr., and D. J. Southwood, Storm-associated Pc5 micropulsation event observed at the synchronous equatorial orbit, *J. Geophys. Res.*, **77**, 143, 1972.
- Bartels, J., Discussion of time variations of geomagnetic activity K_p and A_p , 1932-1961, *Ann. Geophys.*, **19**, 1, 1963.
- Bauer, T. M., W. Baumjohann, and R. A. Treumann, Neutral sheet oscillations at substorm onset, *J. Geophys. Res.*, **100**, 23,737, 1995.
- Baumjohann, W., N. Skopke, J. LaBelle, B. Klecker, H. Lühr, and K. H. Glassmeier, Plasma and field observations of a compressional Pc 5 wave event, *J. Geophys. Res.*, **92**, 12,203, 1987.
- Baumjohann, W., G. Paschmann, and H. Lühr, Characteristics of high-speed ion flows in the plasma sheet, *J. Geophys. Res.*, **95**, 3801, 1990.
- Baumjohann, W., G. Paschmann, T. Nagai, and H. Lühr, Superposed epoch analysis of the substorm plasma sheet, *J. Geophys. Res.*, **96**, 11,605, 1991.
- Borodkova, N. L., G. N. Zastenker, and D. G. Sibeck, A case and statistical study of transient magnetic field events at geosynchronous orbit and their solar wind origin, *J. Geophys. Res.*, **100**, 5643, 1995.
- Cao, M., R. L. McPherron, and C. T. Russell, Statistical study of ULF wave occurrence in the dayside magnetosphere, *J. Geophys. Res.*, **99**, 8731, 1994.
- Chen, L., and A. Hasegawa, A theory of long-period magnetic pulsation, 1, steady state excitation of field line resonance, *J. Geophys. Res.*, **79**, 1024, 1974.
- Coleman, P. J., Jr., Geomagnetic storms at ATS 1, in *Inter-correlated Satellite Observations Related to Solar Events*, edited by V. Manoo and D. E. Page, p. 251, D. Reidel, Norwell, Mass., 1970.
- Cummings, W. D., R. J. O'Sullivan, and P. J. Coleman Jr., Standing Alfvén waves in the magnetosphere, *J. Geophys. Res.*, **74**, 778, 1969.
- Engebretson, M. J., L. J. Zanetti, T. A. Potemra, and M. H. Acuña, Harmonically structured ULF pulsations observed by the AMPTE/CCE magnetic field experiment, *Geophys. Res. Lett.*, **13**, 905, 1986.
- Engebretson, M. J., L. J. Cahill Jr., R. L. Arnoldy, B. J. Anderson, T. J. Rosenberg, D. L. Carpenter, U. S. Inan, and R. H. Eather, The role of the ionosphere in coupling upstream ULF wave power into the dayside magnetosphere, *J. Geophys. Res.*, **96**, 1527, 1991.
- Hamilton, D. C., G. Gloekler, F. M. Ipavich, W. Stüdemann, B. Wilken, and G. Kremser, Ring current development during the great geomagnetic storm of February 1986, *J. Geophys. Res.*, **93**, 14,343, 1988.
- Hasegawa, A., Plasma instabilities and nonlinear effects, in *Physics and Chemistry in Space*, vol. 8, Springer-Verlag, New York, 1975.
- Hasegawa, A., K. H. Tsui, and A. S. Assis, A theory of long period magnetic pulsations, 3, Local field line oscillations, *Geophys. Res. Lett.*, **10**, 765, 1983.
- Hedgecock, P. C., Giant Pc 5 pulsations in the outer magnetosphere: A survey of HEOS-1 data, *Planet. Space Sci.*, **24**, 921, 1976.
- Higbie, P. R., D. N. Baker, R. D. Zwickl, R. D. Belian, J. R.

- Asbridge, J. F. Fennell, B. Wilken, and C. W. Arthur, The global Pc5 event of November 14–15, 1979, *J. Geophys. Res.*, **87**, 2337, 1982.
- Higuchi, T., and S. Kokubun, Waveform and polarization of compressional Pc 5 waves at geosynchronous orbit, *J. Geophys. Res.*, **93**, 14,433, 1988.
- Higuchi, T., S. Kokubun, and S. Ohtani, Harmonic structure of compressional Pc 5 pulsations at synchronous orbit, *Geophys. Res. Lett.*, **13**, 1101, 1986.
- Holter, O., et al., Characterization of low frequency oscillations at substorm breakup, *J. Geophys. Res.*, **100**, 19,109, 1995.
- Holzer, R. E., and J. A. Slavin, Magnetic flux transfer associated with expansions and contractions of the dayside magnetosphere, *J. Geophys. Res.*, **83**, 3831, 1978.
- Joselyn, J. A., Geomagnetic activity forecasting: The state of the art, *Rev. Geophys.*, **33**, 383, 1995.
- Junginger, H., G. Geiger, G. Haerendel, F. Melzner, E. Amata, and B. Higel, A statistical study of dayside magnetospheric electric field fluctuations with periods between 150 and 600 s, *J. Geophys. Res.*, **89**, 5495, 1984.
- Kokubun, S., Characteristics of storm sudden commencement at geostationary orbit, *J. Geophys. Res.*, **88**, 10,025, 1983.
- Kokubun, S., Statistical character of Pc 5 waves at geostationary orbit, *J. Geomagn. Geoelectr.*, **37**, 759, 1985.
- Kokubun, S., K. N. Erickson, T. A. Fritz, and R. L. McPherron, Local time asymmetry of Pc 4-5 pulsations and associated particle modulations at synchronous orbit, *J. Geophys. Res.*, **94**, 6607, 1989.
- Kremser, G., A. Korth, J. A. Fejer, B. Wilken, A. V. Gurevich, and E. Amata, Observations of quasi-periodic flux variations of energetic ions and electrons associated with Pc 5 geomagnetic pulsations, *J. Geophys. Res.*, **86**, 3345, 1981.
- Lanzerotti, L. J., A. Hasegawa, and C. G. Maclennan, Drift mirror instability in the magnetosphere: Particle and field oscillations and electron heating, *J. Geophys. Res.*, **74**, 5565, 1969.
- Lee, L. C., R. K. Albano, and J. R. Kan, Kelvin-Helmholtz instability in the magnetopause-boundary layer region, *J. Geophys. Res.*, **86**, 54, 1981.
- Lühr, H., N. Klöcker, W. Oelschlägel, B. Häusler, and M. Acuña, The IRM fluxgate magnetometer, *IEEE Trans. Geosci. Remote Sens.*, **23**, 259, 1985.
- Matsuoka, H., K. Takahashi, K. Yumoto, B. J. Anderson, and D. G. Sibeck, Observation and modeling of compressional Pi 3 magnetic pulsations, *J. Geophys. Res.*, **100**, 12,103, 1995.
- Miura, A., Simulation of Kelvin-Helmholtz instability at the magnetospheric boundary, *J. Geophys. Res.*, **92**, 3195, 1987.
- Nagano, H., and T. Araki, Long-duration Pc 5 pulsations observed by geostationary satellites, *Geophys. Res. Lett.*, **10**, 908, 1983.
- Nosé, M., T. Iyemori, M. Sugiura, and J. A. Slavin, A strong dawn/dusk asymmetry in Pc5 pulsation occurrence observed by the DE 1 satellite, *Geophys. Res. Lett.*, **22**, 2053, 1995.
- Potemra, T. A., and L. G. Blomberg, A survey of Pc 5 pulsations in the dayside high-latitude regions observed by Viking, *J. Geophys. Res.*, **101**, 24,801, 1996.
- Ruohoniemi, J. M., R. A. Greenwald, K. B. Baker, and J. C. Samson, HF radar observations of Pc 5 field line resonances in the midnight/early morning MLT sector, *J. Geophys. Res.*, **96**, 15,697, 1991.
- Russell, C. T., and R. L. McPherron, Semiannual variation of geomagnetic activity, *J. Geophys. Res.*, **78**, 92, 1973.
- Saka, O., H. Akaki, O. Watanabe, and D. N. Baker, Ground-satellite correlation of low-latitude Pi 2 pulsations: A quasi-periodic field line oscillation in the magnetosphere, *J. Geophys. Res.*, **101**, 15,433, 1996.
- Samson, J. C., and G. Rostoker, Latitude-dependent characteristics of high-latitude Pc 4 and Pc 5 micropulsations, *J. Geophys. Res.*, **77**, 6133, 1972.
- Sanny, J., D. G. Sibeck, and C. T. Russell, A statistical study of transient events in the outer dayside magnetosphere, *J. Geophys. Res.*, **101**, 4939, 1996.
- Shiokawa, K., W. Baumjohann, and G. Haerendel, Braking of high-speed flows in the near-Earth tail, *Geophys. Res. Lett.*, **24**, 1179, 1997.
- Shiokawa, K., et al., High-speed ion flow, substorm current wedge, and multiple Pi 2 pulsations, *J. Geophys. Res.*, **103**, 4491, 1998.
- Singer, H. J., W. J. Hughes, and C. T. Russel, Standing hydromagnetic waves observed by ISEE 1 and 2: Radial extent and harmonic, *J. Geophys. Res.*, **87**, 3519, 1982.
- Southwood, D. J., Some features of field line resonances in the magnetosphere, *Planet. Space Sci.*, **22**, 483, 1974.
- Southwood, D. J., and M. K. Kivelson, Frequency doubling in ultralow frequency wave signals, *J. Geophys. Res.*, **102**, 27,151, 1997.
- Takahashi, K., and B. J. Anderson, Distribution of ULF energy ($f < 80$ mhz) in the inner magnetosphere: A statistical analysis of AMPTE CCE magnetic field data, *J. Geophys. Res.*, **97**, 10,751, 1992.
- Takahashi, K., and R. L. McPherron, Harmonic structure of Pc 3-4 pulsations, *J. Geophys. Res.*, **87**, 1504, 1982.
- Takahashi, K., and R. L. McPherron, Standing hydromagnetic waves in the magnetosphere, *Planet. Space Sci.*, **32**, 1504, 1984.
- Takahashi, K., P. Higbie, and D. N. Baker, Azimuthal propagation and frequency characteristic of compressional Pc 5 waves observed at geostationary orbit, *J. Geophys. Res.*, **90**, 1473, 1985.
- Takahashi, K., C. Z. Cheng, R. W. McEntire, T. A. Potemra, and L. M. Kistler, Observation and theory of Pc 5 waves with harmonically related transverse and compressional components, *J. Geophys. Res.*, **95**, 977, 1990a.
- Takahashi, K., B. J. Anderson, and S. Ohtani, Multisatellite study of nightside transient toroidal waves, *J. Geophys. Res.*, **101**, 24,815, 1996.
- Takahashi, S., T. Iyemori, and M. Takeda, A simulation of the storm-time ring current, *Planet. Space Sci.*, **38**, 1133, 1990b.
- Walker, A. D. M., R. A. Greenwald, W. F. Stuart, and C. A. Green, STARE auroral radar observations of Pc 5 geomagnetic pulsations, *J. Geophys. Res.*, **84**, 3373, 1979.
- Wodnicka, E. B., The magnetic main phase modeling, *Planet. Space Sci.*, **37**, 525, 1989.
- Yumoto, K., and T. Saito, Relation of compressional HM waves at GOES2 to low-latitude Pc 3 magnetic pulsations, *J. Geophys. Res.*, **88**, 10,041, 1983.
- Zhu, X., and M. G. Kivelson, Compressional ULF waves in the outer magnetosphere, I, Statistical study, *J. Geophys. Res.*, **96**, 19,451, 1991.

M. K. Hudson, Department of Physics and Astronomy, Dartmouth College, 6127 Wilder Laboratory, Hanover, NH 03755-3528. (e-mail: maryk@sunset.dartmouth.edu)

M. R. Lessard, Institute for Space Research, Department of Physics and Astronomy, University of Calgary, 2500 University Dr. NW, Calgary, Alberta, Canada, T2M 1N4. (e-mail: lessard@phys.ucalgary.ca)

H. Lühr, GeoForschungsZentrum, Telegrafenberg, Potsdam D-14473, Germany.

(Received June 3, 1998; revised October 27, 1998; accepted November 12, 1998.)